A comprehensive model for the optical transmission for determining the optimal thickness and figure of merit of Al-doped ZnO films as transparent conducting coatings

Abstract

In this work a comprehensive model for the optical transmission as a function of wavelength and thickness of ZnO:Al films deposited on glass substrates by ultrasonic spray pyrolysis, is worked out. The mathematical expression developed for the transmission of the transparent conducting film on a transparent substrate, considers: 1) the interference effects of multiple specular reflections of coherent light from the front and the back of the flat-parallel-sided interfaces film-air and film-glass substrate, 2) the contribution of free carrier concentration (electrons in the conduction band due to Al doping) to the weak absorption in the visible and near-infrared range, 3) the Urbach tail absorption edge at the low wavelength region (< 400 nm), 4) the effect of surface diffuse scattering of light originated by the roughness of these interfaces on the specular reflection and transmission coefficients. The wavelength dependence of the coefficients of reflection and transmission, and the absorption coefficient of the ZnO:Al film in the low absorption-visible region (400-800 nm), were calculated from the formulas derived for the refractive index and extinction coefficient by using a Lorentz-Drude expression to separate the contribution of the bound-electrons and free-electrons, respectively, to the complex dielectric function. The carrier concentration and dc-electrical conductivity of the ZnO:Al films were measured. The fitting of the semi-empirical formula for the optical transmission with the experimental transmission spectrum was quite good and the effects of the different parameters involved in the model was evidenced. Finally, we show that the formulas derived here for the optical transmission can be used for a more precise determination of previously defined figures of merit for these type of films for their use as transparent conductive electrodes as a function of thickness of ZnO:Al. We discuss the correctness of the figures of merits considered and the usefulness of the model for selecting the optimal thickness for a transparent conductive contact.

I. Introduction

Recently, aluminum-doped zinc oxide (ZnO:Al or AZO) thin films deposited by different techniques, have received much attention as transparent conductive coatings (TCCs) for a wide variety of optoelectronic devices such as electroluminescent flat panel displays, solar cells, ultraviolet sensors, etc. [1] [2] [3][4][5][6][7][8][9][10]. For optimal applications of these films as TCCs the optical transmission should be as high as possible but at the same time the sheet resistance should be as low as possible. A common parameter that has been used to evaluate the quality of diverse TCCs deposited on transparent substrates (such as borosilicate, corning or vitreous silica slides), is the figure of merit defined originally by Fraser and Cook [11] as:

$$F = \frac{T}{R_s} \tag{1}$$

where T is the average transmission in the visible wavelength range (400 - 800 nm) and R_s is the sheet resistance defined by $R_s = \frac{1}{\sigma_o l}$, where σ_o is the dc electrical conductivity in $\Omega^{-1}cm^{-1}$ and l is the thickness of the TCC in cm. According to this definition, the ideal TCC should have a figure of merit with a maximum value. However, since both parameters, T and R_s, depend on the TCC thickness an important question to solve has been whether there is an optimal film thickness for which a maximum figure of merit occurs, and how it can be calculated. An attempt to solve this question was made by Haacke [12], by using the Beer's law for expressing the optical transmission of a TCC film in its simplest form as: $T_B = e^{-\alpha l}$, where α is the optical absorption coefficient in cm^{-1}. In this case the figure of merit was also expressed as a function of l in a simple form as: $F_B = \sigma_o l e^{-\alpha l}$. According to this formula it is easily found that the figure of merit of a TCC with a given σ_o and α achieves a maximum value at $l_m = 1/\alpha$, and for this thickness the sheet resistance is $R_s = \alpha/\sigma_o$ and the transmission is $T_B(l = l_m) = e^{-1} = 0.37$. As can be seen, the use of the simplest formula for the optical transmission ($T_B = e^{-\alpha l}$), in Eq. 1 for the figure of merit predicts that the maximum figure of merit occurs at a film thickness which reduces the optical transmission to only 37%, which is unacceptable for most of the applications of a TCC. For example for a TCC with a value of $\alpha = 4 \times 10^2 cm^{-1}$ and $\sigma_o = 10^2\ \Omega^{-1}cm^{-1}$, the thickness for which a maximum figure of merit ($F_{Bmax} = (\sigma_o/\alpha)0.37 = 0.092\ \Omega^{-1}$) is obtained is: $l_{max} = 2.5 \times 10^{-3}\ cm = 25000\ nm$, and although this TCC has a very low sheet resistance; $R_s = 4\ \Omega/square$, it is very thick and it has also a very low transmission (0.37). In order to solve this problem Haacke redefined the figure of merit by [12]:

$$F_H = \frac{T^{10}}{R_s} \tag{2}$$

In this case using the same Beer's formula for the optical transmission ($T_B = e^{-\alpha l}$), the film thickness which maximizes $F_{HB} = \sigma_o l e^{-10\alpha l}$ is now, $l_{max} = \frac{1}{10\alpha}$, and the transmittance for this thickness is $T_B = e^{-0.1} = 0.90$. Thus for the same TCC with $\alpha = 4 \times 10^2 cm^{-1}$ and $\sigma_o = 10^2\ \Omega^{-1}cm^{-1}$, the thickness to obtain the maximum new figure of merit ($F_{HBmax} = \left(\frac{\sigma_o}{10\alpha}\right)(0.9)^{10} = 8.71 \times 10^{-3}\ \Omega^{-1}$), is $l_{max} = 2.5 \times 10^{-4}\ cm = 2500\ nm$, the corresponding sheet resistance is, $R_s = 40\ \Omega/square$., and the transmittance should be of 90%. However this prediction is not realistic because in the practice this TCC is still thick and the optical transmission for a TCC with this thickness is typically below 80%. On the

other hand, the new maximum figure of merit F_{HBmax} is one order of magnitude lower than the original maximum figure of merit: F_{Bmax}. Thus, although the redefined figure of merit has been used in some works to evaluate TCCs [1] [5][8][9] [13], [14], it seems artificial and unsatisfactory for determining the optimal thickness of a suitable TCC.

In order to compare different TCCs, independently of film thickness, other definitions of the figure of merit have been made for TCCs with very small thickness and very low optical absorption, in terms only of the electrical conductivity and the absorption coefficient [15], [16]. However this figure of merit is not valid for thicker or more absorbing films and it does not allow adjusting the optimal thickness for a specific application of the TCC. It is worth to mention that in most of the works where the figure of merit has been calculated or predicted theoretically, it has been implicitly assumed that α is independent of σ_o. However, according to the Drude-Lorentz model, the optical absorption in a TCC is related with the dc-electrical conductivity and/or the free carrier concentration.

As an important motivation for the present work we realize that the use of the simple Beer's formula ($T_B = e^{-\alpha l}$) in the original definition of the figure of merit has given rise to paradox results, because it does not express the real dependence of the optical transmission with film thickness. We consider that the original definition of the figure of merit given by eq. (1) is adequate and can be used in the practice to evaluate the figure of merit of thin and/or thick TCCs, whenever the optical transmission be calculated in a more rigorous form, as a function of the TCC thickness. So, here we have developed a comprehensive semi-empirical model for the optical transmittance (T) of TCC of ZnO:Al films deposited on glass, by ultrasonic spray pyrolysis. For the calculation of T, this model considers the multiple reflections at the three interfaces (air-coating, coating-substrate, substrate-air) and includes: the interference effects of multiple reflections at the coating interfaces, the dispersion formulas for the refractive index of the film and substrate, the effect of free electrons concentration and the roughness of the film surfaces.

II. Model for the specular optical transmittance.

Since the optical transmittance of the films was measured under normal incidence, we used the optical configuration of parallel plates shown in Fig. 1, to model the transmission coefficient through the ZnO:Al film (T_F), and the total transmission coefficient (T) through the whole system ZnO:Al/glass substrate (T). As shown in Fig. 1, the refractive index of the incident medium (air) is $n_0 = 1$, the refractive index of the transparent glass substrate is real and it is denoted by $n_g = n_g(\lambda)$, and the complex refractive index of the film is denoted by $\tilde{n} = \tilde{n}(\lambda) = n(\lambda) + i\kappa(\lambda)$, where the real part, $n(\lambda)$ is called the refractive index and $\kappa(\lambda)$ is the extinction coefficient. Since the ZnO:Al film has a high transparency in the visible range (400 -800 nm), in this range we have weak absorption, where $|\kappa(\lambda)| \ll |n(\lambda)|$.

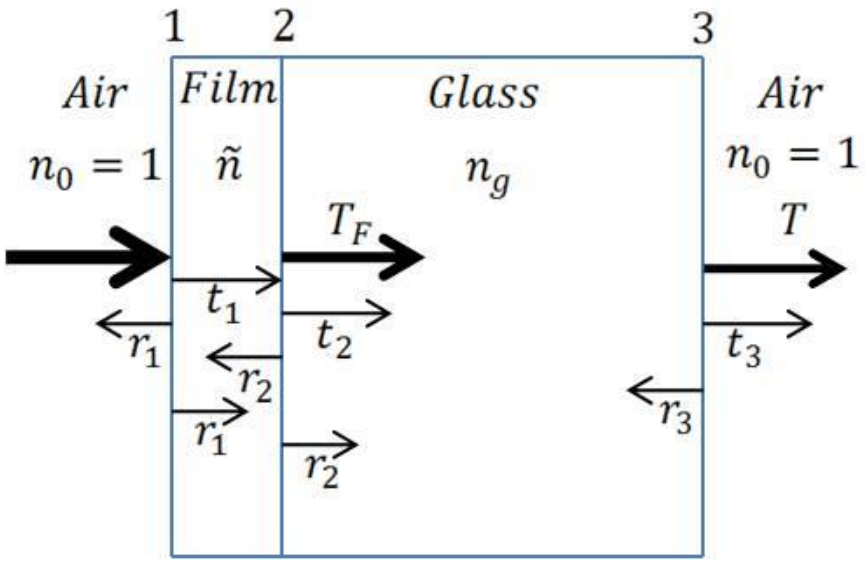

Figure 1. Optical configuration of a ZnO:Al thin film on a thick finite transparent glass substrate. Reprinted with permission from [17] *@ Optica Publishing Group.*

Assuming that the thickness l of the ZnO:Al film is smaller than the coherence length of the light, the interference between multiple reflections inside the film is important [18]. Since the film is deposited on the glass substrate, we have to include the effect of the transparent substrate ($\alpha_S = 0$) in the transmission. The large thickness of the substrate implies the incoherent limit, in which there is no interference among the multiple reflecting beams [18]. Thus, considering the interference effects in the addition of the electric field of the beams transmitted after multiple reflections through the film, and adding the intensities of the multiple reflected beams through the substrate, the transmission through the film/substrate optical system is (see the appendix A) [18]:

$$T = \left[\frac{T_3}{1-R_2'R_3'}\right]\left(\frac{T_1T_2e^{-\alpha l}}{1-2R_1^{1/2}R_2^{1/2}\ cos\,\Phi e^{-\alpha l}+R_1R_2\ e^{-2\alpha l}}\right) \tag{3}$$

where α is the absorption coefficient of the film, $\Phi = 4\pi nl/\lambda$ is the phase shift due to a round-trip of the light wave in the film, λ is the vaccum wavelength of the light, and n is the real part of the complex refractive index of the film. R_1 and R_2 are the internal (inside the film) specular reflectances at the front (1) and back (2) interfaces (assumed ideally flat), respectively (see Fig. 1). R_2' and R_3' are, the specular reflectances inside the substrate, at the substrate-film and substrate–air interfaces, respectively. According to the Fresnel equations, these specular reflectances for weakly absorbing media are expressed as (see the appendix):

$$R_1 = r_1^2 = \left(\frac{n-n_o}{n+n_o}\right)^2 \tag{4}$$

$$R_2 = r_2^2 = \left(\frac{n-n_g}{n+n_g}\right)^2 \tag{5}$$

$$R_2' = r'^2_2 = \left(\frac{n_g-n}{n_g+n}\right)^2 \tag{6}$$

$$R_3^{'} = r'^2_3 = \left(\frac{n_g - n_o}{n_g + n_o}\right)^2 \quad (7)$$

The coefficients of transmission at the three interfaces are expressed as:

$$T_1 = \frac{n}{n_o} t_1^2 = \frac{n}{n_o}\left(\frac{2n_o}{n_o + n}\right)^2 \quad (8)$$

$$T_2 = \frac{n_g}{n} t_2^2 = \frac{n_g}{n}\left(\frac{2n}{n + n_g}\right)^2 \quad (9)$$

$$T_3 = \frac{n_0}{n_g} t_2^2 = \frac{n_0}{n_g}\left(\frac{2n_g}{n_o + n_g}\right)^2 \quad (10)$$

It is worth to mention that the rigorous expression (3) is similar to that used in the past for the determination of the thickness and the optical constants of transparent and weakly absorbing films on transparent substrates [19][20] [21][22] . However in this work we fitted the transmission curve predicted by equation 3, with the experimental transmission obtained for different ZnO:Al films, by introducing the values for the optical constants as a function of wavelength, measured and/or obtained from the models described below, and fitting the film thickness and other parameters such as film roughness and damping constant.

The dependence of the refractive index of the glass substrate with the wavelength was obtained from the experimental spectrum for the interference-free transmission of the glass substrate alone in the absence of film, using the formula [22][23]:

$$n_g = \frac{1}{T_s} + \left(\frac{1}{T_s^2} - 1\right)^{1/2} \quad (11)$$

The refractive index n and extinction coefficient κ of the ZnO:Al film was calculated in terms of the real (ϵ_1) and imaginary (ϵ_2) parts of the complex optical dielectric function $\hat{\epsilon} = \epsilon_1 + i\epsilon_2$, using the well known formulas [18]:

$$n = \frac{1}{\sqrt{2}}\left(\epsilon_1 + (\epsilon_1^2 + \epsilon_2^2)^{1/2}\right)^{1/2} \quad (12)$$

$$\kappa = \frac{1}{\sqrt{2}}\left(-\epsilon_1 + (\epsilon_1^2 + \epsilon_2^2)^{1/2}\right)^{1/2} \quad (13)$$

According to the Drude-Lorentz model the complex optical dielectric function can be expressed as a function of the angular frequency of the light ($\omega = \frac{2\pi c}{\lambda}$) in the following form [6] [18][24]:

$$\hat{\epsilon}(\omega) = \hat{\epsilon}^b + \delta\hat{\epsilon}^f \quad (14)$$

$$\hat{\epsilon}^b = \epsilon_1^b + i\epsilon_2^b = 1 + \frac{Ne^2}{\epsilon_0 m_o}\sum_j \frac{f_j}{\omega_{oj}^2 - \omega^2 - i\gamma_j\omega} \quad (15)$$

$$\delta\hat{\epsilon}^f = \delta\epsilon_1^f + i\delta\epsilon_2^f = -\frac{n_e e^2}{\epsilon_o m(\omega^2 + i\gamma\omega)} \quad (16)$$

This expressions separates explicitly the dielectric function, $\hat{\epsilon}^b$, including only the bound-electrons ($\hat{\epsilon}^b$) of the ZnO lattice with resonant frequencies ω_{oj} and oscillator strengths f_j, and the contribution ($\delta\hat{\epsilon}^f$) of free-electrons (electrons in the conduction band).

In the region of transparency, far from the resonant frequencies, ω_{oj}, the imaginary part, ϵ_2^b, can be considered null and the real part of the optical dielectric function due to bound electrons, ϵ_1^b , can be expressed in the form of a Sellmeier equation [18]. Thus for wavelengths far from the absorption edge of ZnO:Al ($\lambda_{abs} \approx 360\ nm$) we can express

$$\epsilon_2^b = 0 \quad (17)$$

$$\epsilon_1^b = (n^b)^2 = A + \frac{B\lambda^2}{\lambda^2 - C^2} + \frac{D\lambda^2}{\lambda^2 - E^2} \quad (18)$$

with the values of the A, B, C, D and E parameters given in table 1 [25][26].

Table 1. Fitting parameters of Sellmeier model for the refractive index of ZnO thin films [25][26].

A	B	C(nm)	D	E(nm)
2.0065	1.5748×10^6	1.0×10^6	1.5868×10^6	270.63

On the other hand, the explicit expressions for the real and imaginary parts of the free electron contribution are:

$$\delta\epsilon_1^f = -\frac{n_e e^2}{\epsilon_o m(\omega^2 + \gamma^2)} \quad (19)$$

$$\delta\epsilon_2^f = \frac{n_e e^2 \gamma}{\epsilon_o m\omega(\omega^2 + \gamma^2)} \quad (20)$$

where m is the electron mass, ϵ_o is the vacuum permittivity, and $\gamma = \frac{1}{\tau}$ is the damping rate or damping constant, where τ is the free carrier scattering time or relaxation time. Some recent works have shown that the value of the damping constant depends mainly on the frequency or wavelength of the light, but there is also a dependence on the carrier concentration [6][27]. For example, for a ZnO:Al film with a carrier concentration of $3.62 \times 10^{20} cm^{-3}$, the damping constant increases from $1.78 \times 10^{14} Hz$ ($944\ cm^{-1}$) to $2.85 \times 10^{14} Hz$ ($1515\ cm^{-1}$) as the wavelength range of the light increases from the visible region to the infrared region [6]. For larger wavelengths, in the range of terahertz, as the carrier concentration increase from $5.9 \times 10^{17} cm^{-3}$ to $4.0 \times 10^{19} cm^{-3}$ the damping constant increase from $9.2 \times 10^{13} Hz$ to $7.04 \times 10^{14} Hz$ [27].

Thus, substituting the equations (17)-(20) in (14), the real and imaginary parts of the complex optical dielectric function of the ZnO:Al films can be expressed as:

$$\epsilon_1(\lambda) = \epsilon_1^b + \delta\epsilon_1^f = A + \frac{B\lambda^2}{\lambda^2 - C^2} + \frac{D\lambda^2}{\lambda^2 - E^2} - \frac{n_e e^2}{\epsilon_o m(\omega^2 + \gamma^2)} \quad (21)$$

$$\epsilon_2(\lambda) = \epsilon_2^b + \delta\epsilon_2^f = \frac{n_e e^2 \gamma}{\epsilon_o m\omega(\omega^2+\gamma^2)} \quad (22)$$

For the evaluation of these expressions as a function of the wavelength or angular frequency of the light, the concentration of electrons in the ZnO:Al films was measured by Hall effect, as mentioned in the experimental part. The expressions (21) and (22) were used in the formulas (12) and (13) to obtain the wavelength dependence of the refractive index $n(\lambda)$ and extinction coefficient $\kappa(\lambda)$ of the ZnO:Al films. The refractive index was substituted in equations (4) and (5) to calculate the wavelength dependence of the reflection coefficients, R_1 and R_2, for internal specular reflection at the film-air and film-susbstrate interfaces, respectively, which appear in formula (3) for the transmission through the film/substrate optical system. For the absorption coefficient of the ZnO:Al film, that appears in the same formula (3) we considered two contributions. The first contribution was that proportional to the extinction coefficient due to free electrons

$$\alpha_f(\lambda) = \frac{2\kappa(\lambda)\omega}{c} = \frac{4\pi\kappa(\lambda)}{\lambda} \quad (23)$$

where $\kappa(\lambda)$ is the extinction coefficient obtained from the formula (13).

The second contribution was to include the absorption edge of the ZnO:Al film, and it was through an Urbach rule of the absorption edge coefficient, expressed in terms of the energy of the photons $(\hbar\omega)$ and the energy band gap (E_g) of the ZnO:Al film as: $\alpha_U = \alpha_o e^{b(\hbar\omega - E_g)/k_B T_a} = \alpha_o e^{(\hbar\omega - E_g)/E_U}$, where α_o and b are fitting parameters, k_B is the Boltzmann constant and T_a is the absolute temperature in kelvin degrees [18][28]. It must be pointed out that, physically, E_U, is the Urbach energy which is equal to the energy width of the absorption edge and α_o is the convergence value of the absorption coefficient when $\hbar\omega = E_g$ [28]. The exponential increase of the absorption coefficient below the absorption edge is explained by transitions between the tails of density of states in the valence band and the conduction band and the shape and size of these tails depend on the presence of different type of disordering. In terms of the photon wavelength and the absorption edge wavelength which is related to the energy band gap by: $E_g(\text{eV}) = 1240/\lambda_g(nm)$, the Urbach absorption coefficient is commonly expressed as [26][29][30]:

$$\alpha_U(\lambda) = \alpha_o e^{1240\cdot\beta\left(\frac{1}{\lambda}-\frac{1}{\lambda_g}\right)} \quad (24)$$

where α_o and $\beta = 1/E_U$ are fitting parameters.

The band gap of the ZnO:Al films was measured from the absorption edge in the experimental transmission curve (T_{exp}) using the formula for direct interband absorption in a direct band gap semiconductor:

$$\alpha_{exp} = -\frac{1}{d} ln(T_{exp}) \propto (\hbar\omega - E_g)^{1/2} \quad (25)$$

where d is the thickness of the ZnO:Al film and $\hbar\omega$ is the photon energy.

Thus, the absorption coefficient $\alpha(\lambda)$ used in equation (3) was finally expressed by the formula:

$$\alpha(\lambda) = \alpha_f + \alpha_U = \frac{4\pi\kappa(\lambda)}{\lambda} + \alpha_o e^{1240\cdot\beta\left(\frac{1}{\lambda}-\frac{1}{\lambda_g}\right)} \quad (26)$$

At this point it is important to mention that for the deduction of equation (3) it was implicitly assumed that the surfaces of the film and substrate are perfectly smooth. However, according to the AFM and SEM images obtained for various ZnO:Al films (see Figs. 3 and 4), these films have a rough surface, with an average roughness in the range from 15 to 20 nm. As it was shown in an elderly work the specular reflectance of a rough surface is reduced with respect to that of a perfectly smooth surface of the same material [31]. Since then several models have been developed to obtain expressions relating the roughness, σ_s, of a plane surface to the specular reflectance and transmittance at normal incidence, for different magnitudes of the roughness compared with the wavelength, λ [32][33]. Based on these models, in order to include the effect of the surface roughness of the ZnO:Al films in the total transmission, we multiply the specular reflectances at normal incidence of the perfectly smooth surfaces at the front and the back of the films, R_1 and R_2, given by formulas (4) and (5) by a surface scattering factor, to obtain the specular reflectance at the film rough surfaces, expressed as [32]:

$$R_{1rs} = R_1 e^{-\left(2(2\pi n\sigma_s)^2/\lambda^2\right)} \tag{27}$$

$$R_{2rs} = R_2 e^{-\left(2(2\pi n\sigma_s)^2/\lambda^2\right)} \tag{28}$$

In these equations it is assumed that σ_s is the surface roughness at macroscopic level measured by the rms value of the irregularity heights and also that $\sigma_s \ll \lambda$.

In similar way the specular transmittance at the film rough surfaces was expressed as [32], [33]:

$$T_{1rs} = T_1 e^{-\left(\frac{1}{2}\left(2\pi\sigma_{s1}(n_{eff}-1)\right)^2/\lambda^2\right)} \tag{29}$$

$$T_{2rs} = T_2 e^{-\left(\frac{1}{2}\left(2\pi\sigma_{s2}(n_{eff}-1)\right)^2/\lambda^2\right)} \tag{30}$$

In these equation the rough surface of the film was modeled as a thin homogeneous layer with a thickness that is twice the rms roughness of the surface and with an effective refractive index intermediate to the indices of the two adjacent optical media, and in this case (film-air), given by [33]:

$$n_{eff} = \left(\frac{n^2+1}{2}\right)^{1/2} \tag{31}$$

Thus, substituting the expressions (27)-(31) in equation (3), the final expression for the transmittance, including the effect of the roughness, is:

$$T = \left[\frac{T_3}{1-R_2'R_3'}\right]\left(\frac{T_{1rs}T_{2rs}e^{-\alpha l}}{1-2R_{1rs}^{1/2}R_{2rs}^{1/2}\cos\Phi e^{-\alpha l}+R_{1rs}R_{2rs}e^{-2\alpha l}}\right) \tag{32}$$

III. Experimental

The ZnO:Al films modeled in this work were deposited on glass substrates by ultrasonic spray pyrolysis at atmospheric pressure, using the same home-made system, precursor solution and preparation conditions given elsewhere [7]. In this case, the substrate temperature was fixed at 350 °C. A series of ZnO:Al films with different thickness were deposited using different deposition times varying in the range from 5 to 15 min. A double

beam PerkinElmer 35 Uv-Vis spectrometer was used to measure the optical transmission of the films, in the range of wavelengths from 190 to 1100 nm, with a resolution of 1 nm. X-rays diffraction (XRD) measurements were made for determining the crystalline structure of the films, using a Bragg–Brentano Rigaku ULTIMA IV diffractometer with an X-ray source of Cu Ka line (0.15406 nm), at a grazing beam configuration (incidence angle of 1°). The surface morphology of the films was explored by atomic force microscopy (AFM) and scanning electron microscopy (SEM) using a JEOL JSPM-4210 scanning probe microscope and a JEOL 7600F field emission scanning electron microscope (FESEM), respectively. The carrier concentration and electrical conductivity of the films were measured at room temperature by Hall-effect in the van der Pauw configuration, using a Ecopia HMS-3000 system, applying a magnetic field of 0.540 T and a current of 1.0 mA.

IV. Results and discussion

Figure 2 shows the transmission spectra of six ZnO:Al films with different thickness, which were ordered with decreasing thickness (decreasing deposition time) and named AZO1, AZO2, AZO3, AZO4, AZO5 and AZO6, respectively. As can be seen from this figure all the transmission spectra show maxima and minima whose number decreases as the deposition time or thickness of the films decreases.

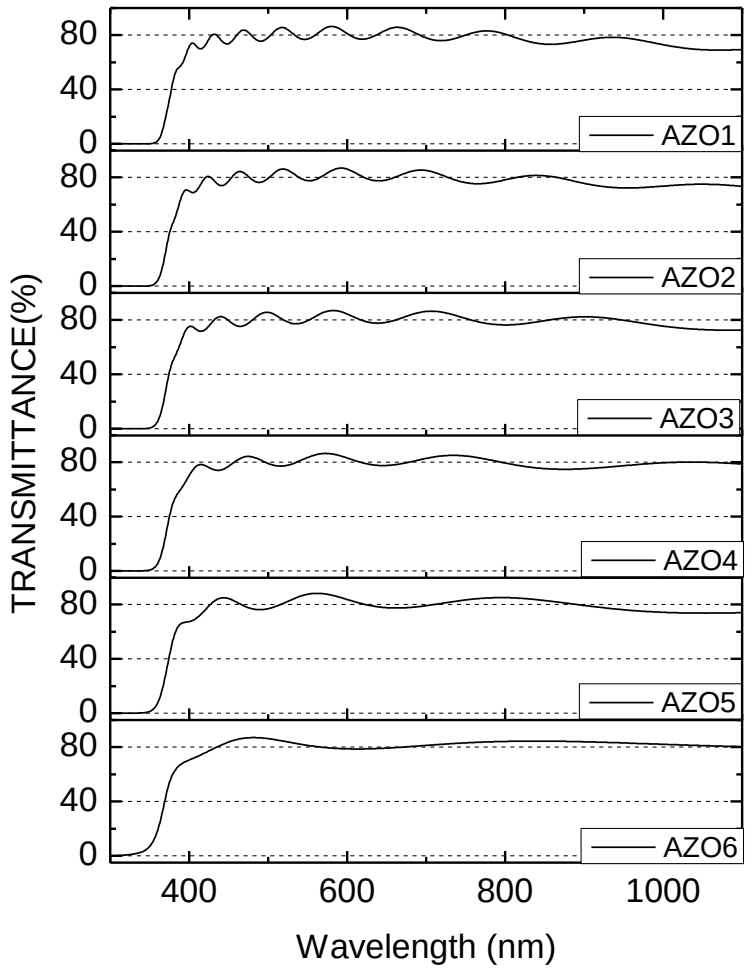

Figure. 2. Experimental optical transmission spectra for ZnO:Al thin films with different thickness deposited on glass substrates. The thickness of the films was decreased from sample AZO1 to sample AZO6, by decreasing the deposition time. Reprinted with permission from [17] @ Optica Publishing Group.

The thickness d of the films was preliminary estimated using the well-known formula obtained from the conditions for the constructive and destructive interference of the multiple reflections of light in the film [19][20] [21][22]: $d = \frac{\lambda_1 \lambda_2}{2(\lambda_1 n(\lambda_1) - \lambda_2 n(\lambda_2))}$, where λ_1 and λ_2 are the wavelengths corresponding to two consecutive maxima (λ_M) or minima (λ_m) of the optical transmission. The thickness of the films can be also calculated from consecutive maxima (λ_M) and minima (λ_m), using the factor 4 instead of the factor 2 in the denominator of the previous formula. For the measurements of the thickness of our AZO films we used the Sellmeier expression for the refractive index, $n(\lambda) = n^b = \sqrt{A + \frac{B\lambda^2}{\lambda^2 - C^2} + \frac{D\lambda^2}{\lambda^2 - E^2}}$, given in equation (18), with the values of the parameters listed in table 1. As it has been shown in some works [22], this formula is not very accurate because in practice it is very sensitive to

variations or non-uniformities in the refractive index and thickness of the films, which give rise to some dispersion in the vales of d. Due this we used the following procedure to estimate the average thickness (d_{av}) for each sample. First, we obtained the average thickness d_{iMm} from the list of wavelengths for consecutive maxima and minima in all the spectral range from 190 to 1100 nm. Then we obtained the average thicknesses d_{iM} and d_{im} from the list of wavelengths for consecutive maxima or consecutive minima, respectively. The average thickness, d_{av}, for each sample was the average of, d_{iMm}, d_{iM} and d_{im}, and all these thicknesses are shown in Table 2.

Table 2. List of estimated thicknesses by the interference formula, along with the carrier concentration, n_e, conductivity, $\boldsymbol{\sigma}$, and sheet resistance, R_{sheet}, and band gap, E_g, experimentally measured for each sample.

Sample	d_{iMm} (nm)	d_{iM} (nm)	d_{im} (nm)	d_{av} (nm)	n_e (cm^{-3})	σ $(\Omega\ cm)^{-1}$	R_{sheet} Ω	E_g (eV) (band gap)
AZO1	1059	1056	1027	1047	$2.7x10^{20}$	$2.08x10^{2}$	45.4	3.41
AZO2	972	947	897	939	$3.02x10^{20}$	$1.98x10^{2}$	51.9	3.42
AZO3	768	758	726	751	$2.54x10^{20}$	$1.46x10^{2}$	91.2	3.43
AZO4	608	600	567	592	$2.6x10^{20}$	$1.24x10^{2}$	136.2	3.40
AZO5	431	437	422	430	$2.22x10^{20}$	$7.9x10^{1}$	293	3.41
AZO6	258	256	-	257	$2.14x10^{20}$	$1.44x10^{2}$	269	3.45

Table 2 also shows the carrier concentration, n_e, conductivity,$\boldsymbol{\sigma}$, and sheet resistance, R_{sheet}, of the films, measured by Hall effect using the van der Pauw configuration. It must be pointed out that we used the average thickness, d_{av}, as the input thickness required for the Hall measurements. The values of the energy band gaps, E_g, of the films listed in table 2 were calculated by taking the plot of $(\alpha_d)^2$ ʋs $\hbar\omega$ obtained from the equation (25) using the experimental transmittance, T_{exp} , and the average film thickness $d = d_{av}$.

The AFM and SEM analysis showed that all the samples have similar morphology. For example, Fig. 3 shows the AFM micrographs and profiles of samples AZO1 and AZO6.

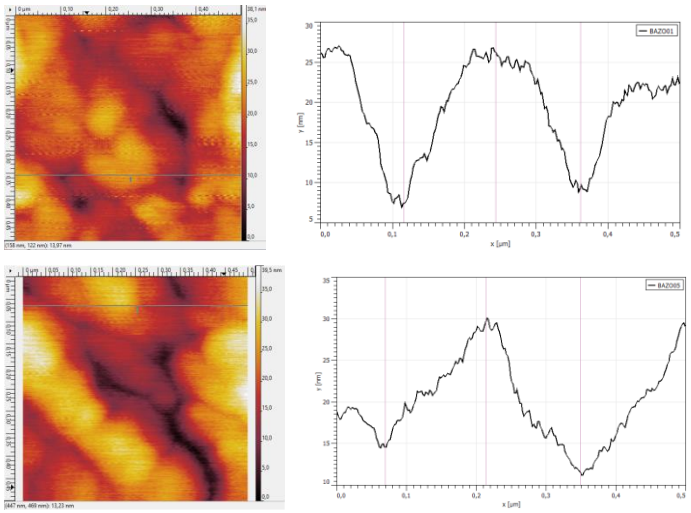

Fig. 2. AFM images and profiles of (a),(b) sample AZO1 and (c),(d) sample AZO6. Reprinted with permission from [17] *@ Optica Publishing Group.*

The AFM profiles of these samples show similar surface heights differences of around 20 nm. Fig. 4 show a cross section FESEM micrograph with a certain rotation and inclination of the AZO1 sample, where it is clearly seen that there is roughness at the top surface and at the bottom surface of the film.

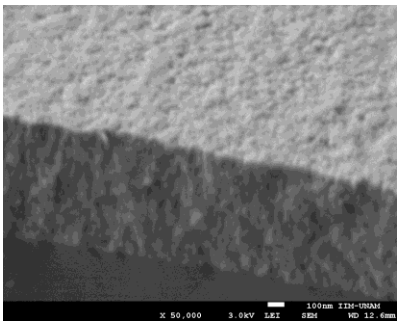

Figure. 4. Cross section FESEM micrograph with a certain rotation and inclination of sample AZO1.

Using the values of carrier concentration, band gap, and average thickness of each film, given in table 2, we started to plot the experimental transmission curves along with the modeled transmission using equation (3) and started to improve the fitting by changing the values of the thickness l appearing in equation (32) around the corresponding average thickness, d_{av}, and adjusting the values of the Urbach parameters, α_o and β. Although we tried the fitting using different constant values of the damping constant, γ, the best fitting was achieved expressing the damping constant as a linear function of the wavelength, as:

$$\gamma = \xi\lambda \tag{33}$$

where ξ was a fitting parameter.

Figure 5 shows the experimental and the best modeled optical transmission for all the samples, using the formula (32), which includes the effect of the roughness at the two interfaces of the films, σ_{s1} and σ_{s2}. As can be seen, the modeled transmission curve fits quite well with the experimental transmission curve, above all in the range of visible wavelengths (400- 800 nm).

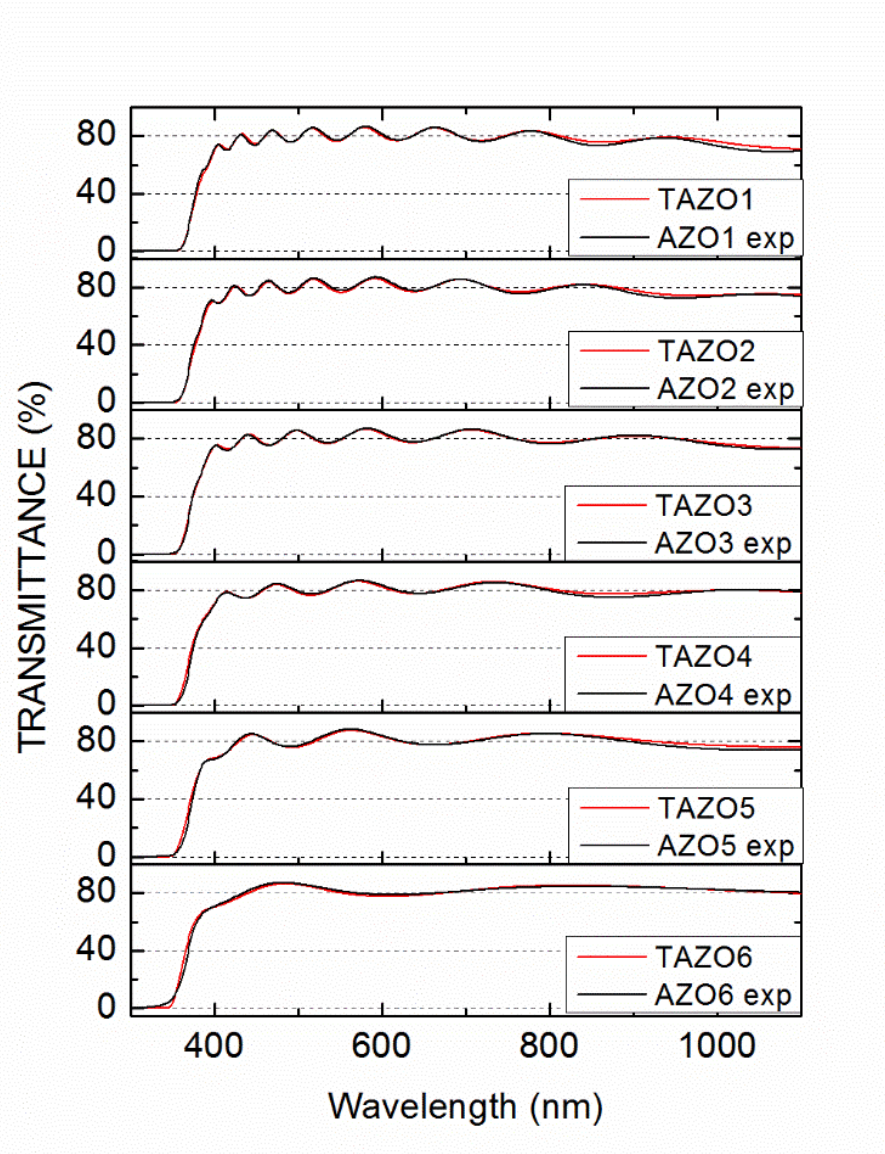

Figure. 5. Experimental (AZO) and the best modeled (TAZO) optical transmission using Eq. (32) for samples AZO1 to AZO6.

Table 3 shows the values of all the parameters which gave rise to the best fitting. Comparing the thicknesses for the fitting, listed in table 3, with the average thicknesses, d_{av}, listed in table 2, we found that the fitting thickness for samples AZO1 –AZO5 is around 2 - 4 % lower than the corresponding average thickness, and for the thinnest sample AZO6, l is 9% lower than d_{av}.

Sample	AZO1	AZO2	AZO3	AZO4	AZO5	AZO6
Average Thickness (nm)	1047	939	751	592	430	257
Thickness l (nm)	1024	900	735	575	424	233
$\boldsymbol{n_e}$ $(\times \mathbf{10^{20}cm^{-3}})$	2.7	3.02	3	2.6	2.22	2.88
$\boldsymbol{\sigma(10^2)}$ $(\Omega \boldsymbol{cm})^{-1}$	2.08	1.98	2.54	1.24	1.53	2.84
$\boldsymbol{\xi}$ $(\times \mathbf{10^{11}\ Hz\ nm^{-1}})$	2.8	2.8	2.8	3.5	4.8	4.8
α_o $(\times \mathbf{10^{-3}nm^{-1}})$	2.5	2.5	3	2.5	3	3.2
β $(\boldsymbol{eV^{-1}})$	10	10	10	10	9.2	10
$\boldsymbol{\lambda_g(nm)}$	363	363	363	364	364	364
σ_{s1}**(nm)**	20	20	20	21	16	16
σ_{s2}**(nm)**	18	18	18	20	16	16

IV.1 Effect of the different parameters on the fitting of the modeled transmittance curves

In this section we show the effect that the different parameters have on the fitting of the modeled transmission curves compared with the experimental ones. Figure 6 a) shows the experimental and the best modeled optical transmission for sample AZO3, meanwhile Fig. 6 b) shows the experimental and the modeled transmission using the corresponding average thickness measured for this sample given in table1 ($d_{Av} = 751nm$), instead of the thickness of $l = 735\ nm$, which gives the best fitting. As can be seen from Fig. 6 b), a change of 2 % in the thickness shifts the wavelength positions of the maxima and minima for the modeled curve with respect to the experimental one. This misfit is expected since the thickness l enters in the formula for the modeled transmittance, which includes the contribution of both, the free electrons and the bound electrons in the dependence of the refractive index of the films with respect to the wavelength, meanwhile the thickness d_{Av} is calculated considering only the contribution of the bound electrons (only the Sellmeier formula). As Fig. 6 c) shows, the effect of neglecting $(n_e = 0)$ the contribution of the free carriers to the refractive index of the films is to increase the modeled transmission with respect to the experimental transmission, mainly in the infrared region, and also to shift the wavelength position of the maxima and minima. This is also expected since $n_e = 0$ implies that there is no optical absorption in the visible and infrared region due to free carriers and only remains the absorption edge in the ultraviolet region due to interband absorption. $n_e = 0$, also implies a change in the refractive index of the film and the consequent shift in the maxima and minima of interference.

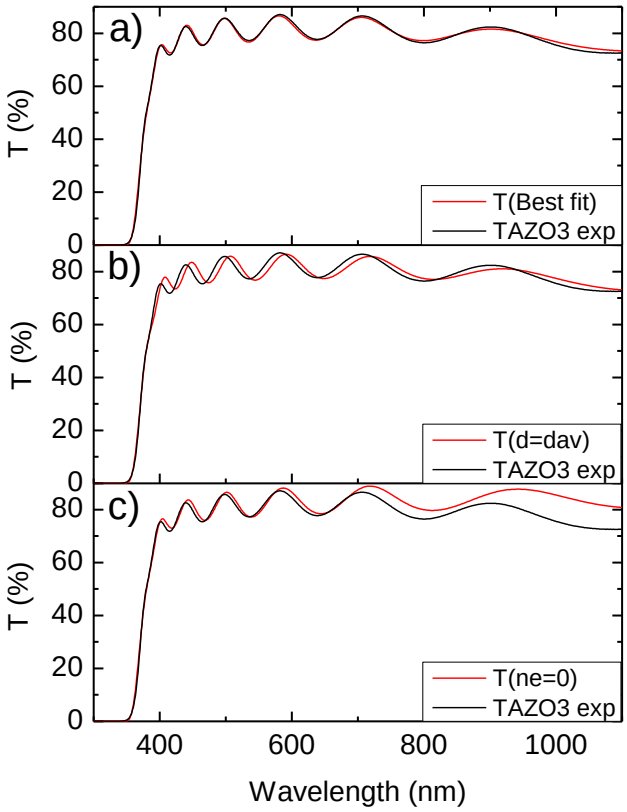

Figure 6. Experimental optical transmission for sample AZO3 and for the same sample: a) the best modeled transmission, b) the modeled transmission using $l = d_{Av} = 751nm$, *and c) the modeled transmission neglecting* $(n_e = 0)$ *the contribution of the free carriers.*

Figure 7 a) and 7 b) show the effect of using a fixed value for the damping constant, γ, of $5 \times 10^{13} Hz$ and $3 \times 10^{14} Hz$, respectively, instead of using the linear dependence given by equation (33) in the modeled transmission for sample AZO3, which gives rise to the value of $5.34 \times 10^{13} Hz$ for $\lambda = 190\, nm$ and $3.08 \times 10^{14} Hz$ for $\lambda = 1100 nm$. As can be seen from Figs. 7 a) and 7 b) a low fixed value of the damping constant gives rise to an increase in the modeled transmission with respect to the experimental transmission, mainly in the infrared region, meanwhile a high fixed value decreases the modeled transmission in the infrared region and even in the visible region. Figure 7 c) shows the effect of removing the roughness from the modeled curve. As can been from this figure, neglecting the roughness, the visibility of the modeled curve (the difference between transmission percentage between maxima and minima) increases with respect to that of the experimental curve. So, as expected, the effect of the roughness is to decrease the visibility of the interference pattern in the transmission curve, mainly in the visible region. It is worth to mention that the rms roughness values listed in table 3, which gave the best fitting of the visibility of the films, are in good agreement with the roughness observed in the AFM profiles of the samples (see Figs 3)

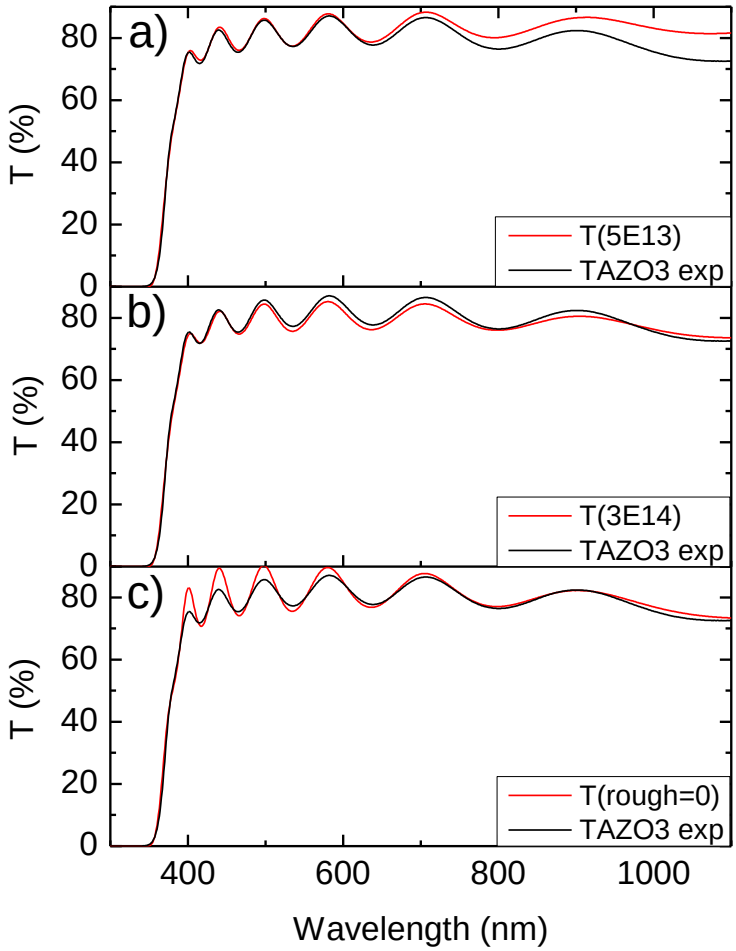

Figure 7. Experimental optical transmission for sample AZO3 and the modeled optical transmission for the same sample using: a) $\gamma = 5 \times 10^{13} Hz$ *, b)* $\gamma = 3 \times 10^{14} Hz$ *, and c)* $\sigma_s = 0$ *, i.e. neglecting the effect of the surface roughness.*

Figure 8 a) shows the effect of changing the value of parameter β in the Urbach rule formula to $\beta = 5\ eV^{-1}$, instead of the value of this parameter for the best fitting of the experimental transmission curve of sample AZO3, which, as shown in table 3 is: $\beta = 10\ eV^{-1}$. As can be seen from this figure, the decrease in the value of this parameter widens the absorption edge in such a way that the AZO film starts to absorb light at a larger wavelength, or equivalently at a lower energy. This is well expected since the Urbach energy is: $E_U = \frac{1}{\beta}$, so, a decrease in the parameter β means an increase in the energy width of the absorption edge, which in turn means a widening of the tails of the density of states above the valence band and below the conduction band [28]. Consequently, the optical absorption due to electron transitions between these tails occurs at lower energies or larger wavelengths. As Fig. 8 b) shows a

decrease in the value of the parameter α_o , from $\alpha_o = 3 \times 10^{-3} nm^{-1}$ (best fit) to $\alpha_o = 1 \times 10^{-3} nm^{-1}$, in the Urbach rule formula has the effect of increasing the optical transmission, just in the region of the absorption edge . This is directly explained by the fact that α_o is the value of the absorption coefficient when $\hbar\omega = E_g$ [28], and a decrease in the value of this coefficient implies an increase in the optical transmittance a wavelengths close to $\lambda_g(nm) = 1240/E_g(\text{eV})$. On the other hand, from this last relation between λ_g and the band gap E_g, it is evident why an increase in the absorption wavelength parameter, from $\lambda_g = 363\, nm$ (best fit) to $\lambda_g = 370\, nm$, shifts the transmittance curve to larger wavelengths, as observed in Fig. 8 c)

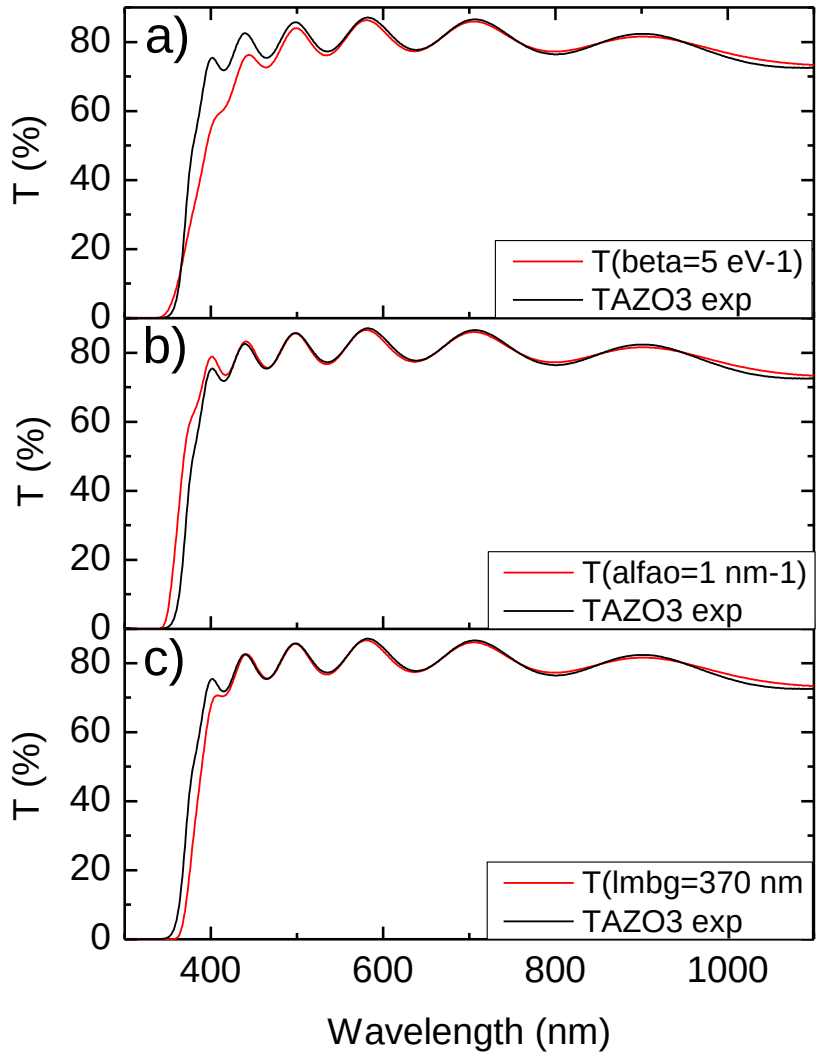

Figure 8. Experimental optical transmission for sample AZO3 and the modeled optical transmission for the same sample using: a) $\beta = 5\ eV^{-1}$, b) $\alpha_o = 1 \times 10^{-3} nm^{-1}$, and c) $\lambda_g = 370\ nm$.

IV.2 Figure of merit and criteria to choose the best TCC.

In this section we use the rigorous expression (32) for the transmission of a ZnO:Al thin film on a glass substrate, with the parameters for the best fit for sample AZO3, to calculate and/or predict the average optical transmission, in the visible range from 400 to 800 nm, as a function of thickness, assuming thicknesses in the range from 50 nm to 10000 nm. Using the average value of the absorption coefficient in the same visible range, $\bar{\alpha} = 3.45 \times 10^{-5} nm^{-1}$, we also calculated the Beer's transmittance as a function of thickness ($T_B = e^{-\bar{\alpha} l}$). Along with this we calculated the sheet resistance as a function of thickness, $R_s = 1/\sigma_o l$, assuming that the dc-electrical conductivity, σ_o, of the film remains constant in the value measured for sample AZO3 listed in table 1, $\sigma_o = 146\ \Omega^{-1}\text{cm}^{-1}$. Figure 9 shows the plot of the modeled optical transmission, T, the Beer´s transmission, T_B , and the sheet resistance as a function of thickness. As can be seen, the sheet resistance decrease hyperbolically with thickness, meanwhile both transmissions, T and T_B decrease almost linearly with increasing the thickness in the range of 50 to 10000 nm. This cuasi-linear decrease is because in this range of thicknesses the factor $\bar{\alpha} l$ is small. However, the modeled transmission is around 20% lower than the unrealistic Beer's transmission T_B.and the latter decreases with o lower slope than the former.

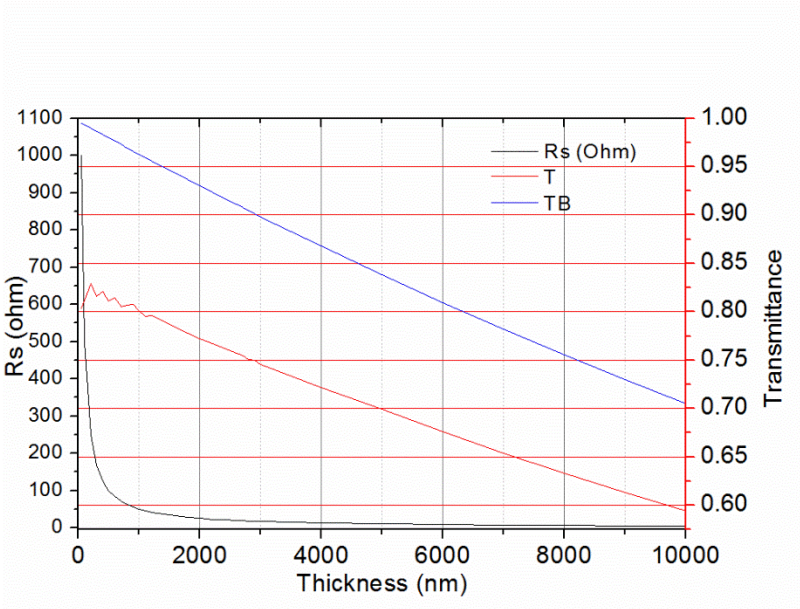

Figure 9. Plots of the modeled optical transmission, T, the Beer´s transmission, T_B , and the sheet resistance, R_S , as a function of thickness.

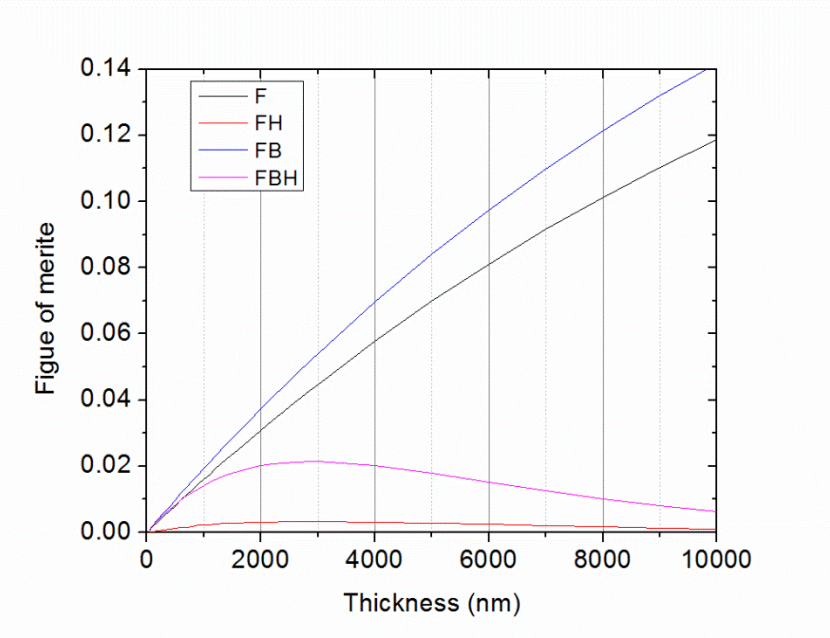

Figure 10. Plots of original figures of merit using the modeled trasnmisssion ($F = \frac{T}{R_s}$) and the Beer´s transmission ($F_B = \frac{T_B}{R_s}$), and the redefined Figures of merit by Haacke, $F_H = \frac{T^{10}}{R_s}$ and $F_{HB} = \frac{T_B^{10}}{R_s}$. Reprinted with permission from [17] *@ Optica Publishing Group.*

Based on the definitions given by equations (1) and (2) for the original figure of merit and the redefined Figure of merit by Haacke, respectively, we calculated these figures of merit as a function of thickness, using both, the modeled trasnmisssion and the Beer´s transmission. Figure 10 shows the plots of these figures of merit, and as can be seen the original figures of merit, $F = \frac{T}{R_s}$ and $F_B = \frac{T_B}{R_s}$, are far from reaching the maximum value, for the region of thickness considered in the plot. This was expected since based on the discussion given in the introduction, this maximum value should be reached for a thickness equal to $l = \frac{1}{\bar{\alpha}} = \frac{1}{3.45\times10^{-5}nm^{-1}} \approx 28985\ nm$. This shows clearly that the criteria of choosing a thin film of ZnO:Al with this thickness, as the best TCC is unrealistic, even using the modeled transmission. On the other hand, as the same Fig. 10 shows, the redefined figures of merit, $F_H = \frac{T^{10}}{R_s}$ and $F_{HB} = \frac{T_B^{10}}{R_s}$, do reach the maximum value of $\sim 3 \times 10^{-3}\Omega^{-1}$ and $2 \times 10^{-2}\Omega^{-1}$, respectively, for a thickness $l \approx 2900\ nm$. Although this thickness is much lower, it is still questionable to choose this as the thickness for a ZnO:Al thin film to be the best TCC. As Fig. 9 shows, in spite of the fact that this film would have a very low sheet resistance of $\sim 17\ \Omega$, its transmission would be $T \approx 0.75$, which do not meet the general criteria of $T \geq 0.80$ to be considered a good TCC [34]. As Fig. 9 shows, in order to meet this criteria the thickness of the film should be: $l \approx 1000\ nm$, and this film would have a sheet resistance of $\sim 50\ \Omega$, and a figure of merit of $1.6 \times 10^{-2}\Omega^{-1}$. From this analysis we can conclude that the criteria of choosing the thickness of the best TCC film as that to get the maximum of the original or the redefined figure of merit, is not a realistic criteria. The

alternative method proposed in this work to determine the thickness of a ZnO:Al film, for its application as a good TCC, is to select this thickness from the plots shown in Fig 10 of the sheet resistance and the average transmission calculated from our modeled transmission, in the region of thicknesses where this average transmission is equal or higher than 80 %. From these plots it is clearly seen that in order to obtain TCCs with sheet resistances between 100 and 50 Ω, the thickness of the ZnO:Al films must be in the range from 500 to 1000 nm, and the figure of merit of this TCCs have values in the range from 8.1×10^{-3} to 1.16×10^{-2} Ω^{-1}.

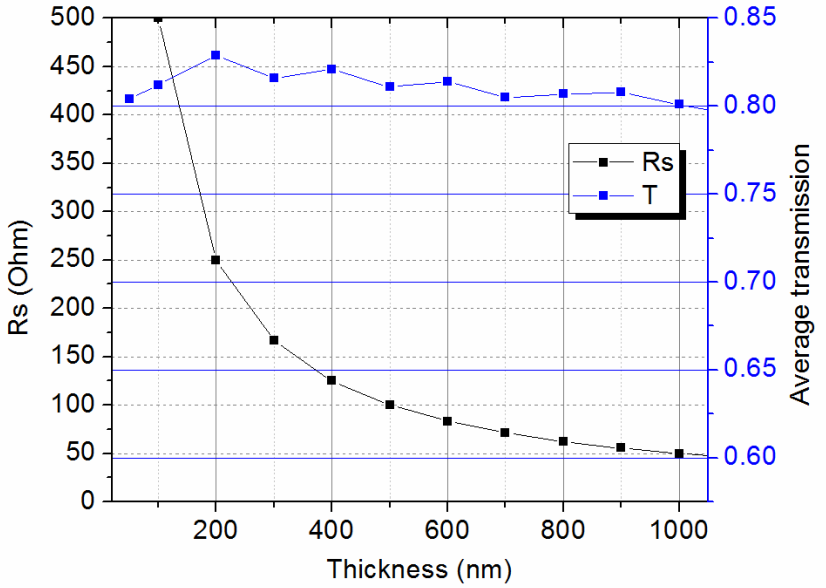

Figure 11. Plots of sheet resistance and average transmission calculated from the modeled transmission, in the region of thicknesses where this average transmission is equal or higher than 80%. *Reprinted with permission from* [17] *@ Optica Publishing Group.*

V. Conclusions

We have developed a comprehensive expression for the optical transmission of thin films of ZnO:Al deposited by ultrasonic spray pyrolysis on glass substrates, with the purpose of calculating their figure of merit and their optimal thickness as TCCs. The modeled transmission considers the effect of the free carrier concentration, measured by Hall effect, in the optical absorption of the films, as well as the Urbach absorption edge, the interference effects of multiple specular reflections and roughness of the film's surfaces. Our results show that by fitting the model presented here to the experimental transmission curves for films, very precise values of the thickness and rms roughness of the films can be obtained, as well as the values of some important optical and electronic parameters such as the band gap and width of the energy band tails associated to the conduction and valence bands.

Appendix A

The expression (3) for the transmission T through the system air/film/glass substrate/air shown in Fig 1 is derived in this appendix.

We assume that the refractive index of air is real ($n_0 = 1$), the refractive index of the film is complex $\left(\tilde{n} = n(\lambda) + i\kappa(\lambda)\right)$, and the refractive index of the glass substrate is real $n_g = n_g(\lambda)$. The spatial component of the electric field of one plane wave propagating in the x direction (at normal incidence of the light beam with the film surface) inside the film of thickness l can be expressed as:

$$E_f = E_{tf} e^{i\tilde{k}x} \qquad (A1)$$

where $0 \le x \le l$, $E_{tf}$is the electric field of the transmitted wave at the interface 1 air-film ($x = 0$) and

$$\tilde{k} = \tilde{n}\frac{\omega}{c} = \tilde{n}\frac{2\pi}{\lambda} \qquad (A2)$$

where λ is the wavelength of the light in air~vacuum.

According to Fresnel's relations, at normal incidence, the amplitude transmission coefficients at the air-film (1) and film-substrate (2) are, respectively:

$$\tilde{t}_1 = \left(\frac{E_{0t1}}{E_{01}}\right) = \frac{2n_o}{n_o + \tilde{n}} \qquad (A3)$$

$$\tilde{t}_2 = \left(\frac{E_{0t2}}{E_{02}}\right) = \frac{2\tilde{n}}{\tilde{n} + n_g} \qquad (A4)$$

and the corresponding amplitude reflection coefficients are:

$$\tilde{r}_1 = \left(\frac{E_{0r1}}{E_{01}}\right) = \frac{n_o - \tilde{n}}{n_o + \tilde{n}}$$

$$\tilde{r}_2 = \left(\frac{E_{0r2}}{E_{02}}\right) = \frac{\tilde{n} - n_g}{\tilde{n} + n_g}$$

Let us assume that the coherence length of light exceeds the thickness, *l*, of the film and thus, the interference effects of the multiply reflected beams are important. So considering multiple reflections, the electric field of the first, second, and the m-th beam transmitted through the film (from the air toward the glass substrate) are, respectively:

$$E_{tf1} = E_0 \tilde{t}_1 \tilde{t}_2 e^{i\tilde{n}\frac{2\pi}{\lambda}l} = E_0 \tilde{t}_1 \tilde{t}_2 \, e^{i\tilde{Q}}$$

$$E_{tf2} = \left[E_0 \tilde{t}_1 \tilde{t}_2 e^{i\tilde{Q}}\right] \tilde{r}_1 \tilde{r}_2 \, e^{i2\tilde{Q}}$$

$$\ldots\ldots\ldots\ldots\ldots\ldots\ldots\ldots\ldots\ldots\ldots\ldots$$

$$E_{tm} = \left[E_0 \tilde{t}_1 \tilde{t}_2 e^{i\tilde{Q}}\right] \tilde{r}_1^{\,m-1} \tilde{r}_2^{\,m-1} e^{i2(m-1)\tilde{Q}}$$

where

$$\tilde{Q} = \tilde{n}\frac{2\pi}{\lambda}l$$

Adding all the terms from $m = 1$ to $m \to \infty$ and redefining the index $k = m - 1$

$$E_T = \left[E_0 \tilde{t}_1 \tilde{t}_2 e^{i\tilde{Q}}\right] \sum_{k=0}^{\infty} \left(\tilde{r}_1 \tilde{r}_2 e^{i2\tilde{Q}}\right)^k$$

Then using

$$\tilde{q} = \tilde{r}_1 \tilde{r}_2 e^{i2k\tilde{Q}} < 1$$

$$\sum_{k=0}^{\infty} \left(\tilde{r}_1 \tilde{r}_2 e^{i2\tilde{Q}}\right)^k = \sum_{k=0}^{\infty} \tilde{q}^k = \frac{1}{1-\tilde{q}} = \frac{1}{1 - \tilde{r}_1 \tilde{r}_2 e^{i2\tilde{Q}}}$$

we obtain,

$$\tilde{t} = \frac{E_T}{E_0} = \frac{\tilde{t}_1 \tilde{t}_2 e^{i\tilde{Q}}}{1 - \tilde{r}_1 \tilde{r}_2 e^{i2\tilde{Q}}}$$

Separating the real part and the imaginary parts of $\tilde{Q}$,

$$\tilde{Q} = \frac{\Phi}{2} + \mathrm{i}\alpha/2$$

where

$$\alpha = \frac{4\pi\kappa}{\lambda},$$

and,

$$\Phi = \frac{4\pi n}{\lambda} l.$$

Therefore,

$$\tilde{t} = \frac{\tilde{t}_1 \tilde{t}_2 e^{-\alpha l/2} e^{-i\Phi/2}}{1 - \tilde{r}_1 \tilde{r}_2 e^{i\Phi} e^{-\alpha l}},$$

and thus,

$$|\tilde{t}|^2 = \frac{|\tilde{t}_1|^2 |\tilde{t}_2|^2 \, e^{-\alpha l}}{|1 - \tilde{r}_1 \tilde{r}_2 e^{i\Phi} e^{-\alpha l}|^2}.$$

In the region of low absorption $|\kappa(\lambda)| \ll |n(\lambda)|$

$$\tilde{r}_1 \cong r_1 = \frac{n_0 - n}{n_0 + n},$$

$$\tilde{r}_2 \cong r_2 = \frac{n - n_g}{n + n_g},$$

$$\tilde{t}_1 \cong t_1 = \frac{2n_o}{n_o + n},$$

and

$$\tilde{t}_2 \cong t_2 = \frac{2n}{n + n_g}.$$

Therefore

$$|\tilde{t}|^2 = \frac{|t_1|^2|t_2|^2\, e^{-\alpha l}}{1 - 2r_1 r_2\ cos\,\Phi\, e^{-\alpha l} + r_1^2 r_2^2\, e^{-2\alpha l}}$$

On the other hand, the intensity or flux of energy of a plane electromagnetic wave in any non-magnetic material is equal to the magnitude of the Poynting vector:

$$I_m = \left|\vec{S}_m\right| = \left|\vec{E}\right|\left|\vec{H}\right| = \frac{n_m}{\mu_o c}\left|\vec{E}\right|^2$$

where n_m is the real part of the refractive index of the non-magnetic material.

Now, the transmittance through the film T_f is the ratio of the transmitted intensity to the incident intensity, that is,

$$T_f = \frac{n_g E_T^2}{n_0 E_0^2} = \frac{n_g}{n_0}|\tilde{t}|^2.$$

Finally, substituting the expression for $|\tilde{t}|^2$ and using $R_1 = r_1^2$ and $R_2 = r_2^2$ yields

$$T_f = \frac{n_g}{n_0}|t_1|^2|t_2|^2 \frac{e^{-\alpha l}}{1 - 2R_1^{1/2}R_2^{1/2}\ \cos\Phi\, e^{-\alpha l} + R_1 R_2\, e^{-2\alpha l}}$$

On the other hand, the transmittance from air to the film is,

$$T_1 = \frac{n}{n_o}t_1^2 = \frac{n}{n_o}\left(\frac{2n_o}{n_o + n}\right)^2,$$

whereas the transmittance from the film to the substrate is,

$$T_2 = \frac{n_g}{n}t_2^2 = \frac{n_g}{n}\left(\frac{2n}{n + n_g}\right)^2.$$

Thus, the transmittance from the air to the glass through the film is,

$$T_f = \frac{T_1 T_2 e^{-\alpha l}}{1 - 2R_1^{1/2}R_2^{1/2}\ cos\,\Phi\, e^{-\alpha l} + R_1 R_2\, e^{-2\alpha l}}$$

Since the thickness of the glass substrate is too large, considering incoherent multiple reflections, the transmission through the glass substrate with $\alpha_g = 0$ is

$$T = T_f \frac{T_3}{1 - R_2 R_3}$$

Where

$$T_3 = \frac{n_0}{n_g}\left(\frac{2n_g}{n_o + n_g}\right)^2$$

and

$$R_3 = r_3^2 = \left(\frac{n_g - 1}{n_g + 1}\right)^2$$

References:

[1] M. Acosta, J. Mendez-Gamboa, I. Riech, C. Acosta, and M. Zambrano, "AZO/Ag/AZO multilayers electrodes evaluated using a photonic flux density figure of merit for solar cells applications," *Superlattices Microstruct.*, vol. 127, pp. 49–53, 2019, doi: 10.1016/j.spmi.2018.03.018.

[2] S. O. El Hamali, W. M. Cranton, N. Kalfagiannis, X. Hou, R. Ranson, and D. C. Koutsogeorgis, "Enhanced electrical and optical properties of room temperature deposited Aluminium doped Zinc Oxide (AZO) thin films by excimer laser annealing," *Opt. Lasers Eng.*, vol. 80, pp. 45–51, 2016, doi: 10.1016/j.optlaseng.2015.12.010.

[3] S. Singh, "Al doped ZnO based metal-semiconductor-metal and metal-insulator-semiconductor-insulator-metal UV sensors," *Optik (Stuttg).*, vol. 127, no. 7, pp. 3523–3526, 2016, doi: 10.1016/j.ijleo.2016.01.012.

[4] C.-H. Zhai *et al.*, "Effects of Al Doping on the Properties of ZnO Thin Films Grown by Atomic Layer Deposition," *Nanoscale Res. Lett.*, vol. 11, pp. 407–414, 2016, doi: 10.1021/jp2023567.

[5] O. Gençyılmaz, F. Atay, and I. Akyü, "Deposition and Ellipsometric Characterization of Transparent Conductive Al-doped ZnO for Solar Cell Application," *J. Clean Energy Technol.*, vol. 4, no. 2, pp. 90–94, 2016, doi: 10.7763/JOCET.2016.V4.259.

[6] V. Romanyuk *et al.*, "Optical and electrical properties of highly doped ZnO:Al films deposited by atomic layer deposition on Si substrates in visible and near infrared region," *Acta Phys. Pol. A*, vol. 129, no. 1, pp. A36–A40, 2016, doi: 10.12693/APhysPolA.129.A36.

[7] M. J. Rivera *et al.*, "Low temperature-pyrosol-deposition of aluminum-doped zinc oxide thin films for transparent conducting contacts," *Thin Solid Films*, vol. 605, pp. 108–115, 2016, doi: 10.1016/j.tsf.2015.11.053.

[8] M. L. Grilli, A. Sytchkova, S. Boycheva, and A. Piegari, "Transparent and conductive Al-doped ZnO films for solar cells applications," *Phys. Status Solidi*

Appl. Mater. Sci., vol. 210, no. 4, pp. 748–754, 2013, doi: 10.1002/pssa.201200547.

[9] A. Sytchkova *et al.*, "Radio frequency sputtered Al:ZnO-Ag transparent conductor: A plasmonic nanostructure with enhanced optical and electrical properties," *J. Appl. Phys.*, vol. 114, no. 9, 2013, doi: 10.1063/1.4820266.

[10] K. Ellmer, "Past achievements and future challenges in the development of optically transparent electrodes," *Nat. Photonics*, vol. 6, no. 12, pp. 809–817, 2012, doi: 10.1038/nphoton.2012.282.

[11] D. B. Fraser and H. D. Cook, "Highly Conductive, Transparent Films of Sputtered In[sub 2−x]Sn[sub x]O[sub 3−y]," *J. Electrochem. Soc.*, vol. 119, no. 10, pp. 1368–1374, 1972, doi: 10.1149/1.2403999.

[12] G. Haacke, "New figure of merit for transparent conductors," *J. Appl. Phys.*, vol. 47, no. 9, pp. 4086–4089, 1976, doi: 10.1063/1.323240.

[13] K. Sivaramakrishnan, N. D. Theodore, J. F. Moulder, and T. L. Alford, "The role of copper in ZnO/Cu/ZnO thin films for flexible electronics," *J. Appl. Phys.*, vol. 106, no. 6, pp. 0635101–0635108, 2009, doi: 10.1063/1.3213385.

[14] H. W. Wu, R. Y. Yang, C. M. Hsiung, and C. H. Chu, "Influence of Ag thickness of aluminum-doped ZnO/Ag/aluminum-doped ZnO thin films," *Thin Solid Films*, vol. 520, no. 24, pp. 7147–7152, 2012, doi: 10.1016/j.tsf.2012.07.124.

[15] R. G. Gordon, "Criteria for Choosing Transparent Conductors," *MRS Bull.*, vol. 25, no. 08, pp. 52–57, 2000, doi: 10.1557/mrs2000.151.

[16] V. K. Jain and A. P. Kulshreshtha, "Indium-tin-oxide transparent conducting coatings on silicon solar cells and their figure of merit," *Sol. Energy Mater.*, vol. 4, pp. 151–158, 1981.

[17] B. Juárez-García, J. González-Gutiérrez, M. J. Rivera-Medina, A. García-Valenzuela, and J. C. Alonso-Huitrón, "Requirements and applications of accurate modeling of the optical transmission of transparent conducting coatings," *Appl. Opt.*, vol. 58, no. 19, p. 5179, 2019, doi: 10.1364/ao.58.005179.

[18] M. Fox, *Optical properties of Solids*, Second Ed. Oxford University Press, 2010.

[19] J. C. Manifacier, J. Gasiot, and J. P. Fillard, "A simple method for the determination of the optical constants n, k and the thickness of a weakly absorbing thin film," *J. Phys. E.*, vol. 9, no. 11, pp. 1002–1004, 1976, doi: 10.1088/0022-3735/9/11/032.

[20] A. M. Goodman, "Optical interference method for the approximate determination of refractive index and thickness of a transparent layer.," *Appl. Opt.*, vol. 17, no. 17, pp. 2779–2787, 1978, doi: 10.1364/AO.17.002779.

[21] G. D. Cody, C. R. Wronski, B. Abeles, and E. Company, "Optical Characterization of Amorphous Silicon Hydride Films," *Sol. Cells*, vol. 2, no. 3, pp. 227–243, 1980.

[22] R. Swanepoel, "Determination of the thickness and optical constants of amorphous Ge-Se-Bi thin films," *J. Phys. E Sci. Instrum.*, vol. 16, pp. 1–10, 1983, doi: 10.1080/14786430902835644.

[23] M. D. Wang *et al.*, "Determination of thickness and optical constants of ZnO thin films prepared by filtered cathode vacuum arc deposition," *Chinese Phys. Lett.*, vol. 25, no. 2, pp. 743–746, 2008, doi: 10.1088/0256-307X/25/2/106.

[24] A. D. Rakić, A. B. Djurišić, J. M. Elazar, and M. L. Majewski, "Optical properties of metallic films for vertical-cavity optoelectronic devices," *Appl. Opt.*, vol. 37, no. 22, pp. 5271–5283, 1998, doi: 10.1364/AO.37.005271.

[25] X. W. Sun and H. S. Kwok, "Optical properties of epitaxially grown zinc oxide films on sapphire by pulsed laser deposition," *J. Appl. Phys.*, vol. 86, no. 1, pp. 408–411, 1999, doi: 10.1063/1.370744.

[26] N. B. Khelladi and N. E. C. Sari, "Optical Properties of ZnO Thin Film," *Adv. Mater. Sci.*, vol. 13, no. 1, pp. 21–29, 2013, doi: 10.2478/adms-2013-0003.

[27] J. Tang *et al.*, "Determination of carrier concentration dependent electron effective mass and scattering time of n-ZnO thin film by terahertz time domain spectroscopy," *J. Appl. Phys.*, vol. 115, no. 3, 2014, doi: 10.1063/1.4861421.

[28] I. Studenyak, M. Kranj, and M. Kurik, "Urbach Rule in Solid State Physics," *Int. J. Opt. Appl.*, vol. 4, no. 3, pp. 76–83, 2014, doi: 10.5923/j.optics.20140403.02.

[29] J. M. Khoshman and M. E. Kordesch, "Optical characterization of sputtered amorphous aluminum nitride thin films by spectroscopic ellipsometry," *J. Non. Cryst. Solids*, vol. 351, no. 40–42, pp. 3334–3340, 2005, doi: 10.1016/j.jnoncrysol.2005.08.009.

[30] R. Capan, N. B. Chaure, a. K. Hassan, and a. K. Ray, "Optical dispersion in spun nanocrystalline titania thin films," *Semicond. Sci. Technol.*, vol. 19, pp. 198–202, 2004, doi: 10.1088/0268-1242/19/2/012.

[31] H. E. Bennet and P. O. Porteus, "Relation Between Surface Roughness and Specular Reflectance at Normal Incidence," *J. Opt. Soc. Am.*, vol. 51, no. 2, pp. 123–128, 1961.

[32] P. B. Nagy and L. Adler, "Surface roughness induced attenuation of reflected and transmitted ultrasonic waves," *The Journal of the Acoustical Society of America*, vol. 82, no. 1. pp. 193–197, 1987. doi: 10.1121/1.395545.

[33] C. K. Carniglia and D. G. Jensen, "Single-layer model for surface roughness.," *Appl. Opt.*, vol. 41, no. 16, pp. 3167–3171, 2002, doi: 10.1364/AO.41.003167.

[34] M. Huang, Z. Hameiri, H. Gong, W. C. Wong, A. G. Aberle, and T. Mueller, "Novel hybrid electrode using transparent conductive oxide and silver nanoparticle mesh for silicon solar cell applications," *Energy Procedia*, vol. 55, pp. 670–678, 2014, doi: 10.1016/j.egypro.2014.08.043.